Structure- and Orientation-Dependent Magnetic Susceptibility of Tetramethylammonium Nickel Nitrite, $(CH_3)_4N[Ni(NO_2)_3]$: An $S = 1$ One-Dimensional Heisenberg Antiferromagnet

Liang-Kuei Chou, Khalil A. Abboud, and Daniel R. Talham*

Department of Chemistry, University of Florida, Gainesville, Florida 32611

W. W. Kim and Mark W. Meisel*

Department of Physics, Center for Ultralow Temperature Research, University of Florida, Gainesville, Florida 32611

Received May 10, 1994®

The crystal structure of tetramethylammonium nickel nitrite, $(CH_3)_4N[Ni(NO_2)_3]$ (TMNIN), has been determined; space group $P\bar{3}m1$ with $a = b = 9.1029(7)$ Å, $c = 7.0816(7)$ Å, $V = 508.18(8)$ Å^3 ($\mu = 1.93$ mm^{-1}, $d_{calc} = 1.770$ g/cm^3, $Z = 2$, Mo Kα ($\lambda = 0.710\ 73$ Å), $T = 298$ K). Refinement from 359 reflections with $I > 2\sigma(I)$ and 45 parameters yielded values for R and wR of 2.50 and 2.82, respectively. The structure consists of infinite chains of Ni^{2+} ions with adjacent Ni ions bridged by three cis-μ-nitro ligands such that alternate Ni ions are chemically distinct with Ni1 octahedrally coordinated with six nitrite nitrogens, and the adjacent Ni2 octahedrally coordinated with six nitrite oxygens. The tetramethylammonium ions are located in positions along the 3-fold rotation axes and form channels that separate the Ni chains. The intrachain Ni–Ni distance is 3.541 Å and the interchain separation is 9.1029 Å. Magnetic susceptibility data are presented from 1.8 to 300 K on a sample of aligned single crystals and yield a nearly isotropic nearest-neighbor exchange, $J/k_B \approx -10$ K. From the anisotropy in the g value, a coarse estimate of the axial single ion anisotropy, D, yields $D/k_B \approx 0.5 \pm 1.2$ K. Since TMNIN is an $S = 1$ one-dimensional Heisenberg antiferromagnet, the implications of the alternating chain structure on the existence of a Haldane gap in this material are discussed.

Introduction

The chemical realization of quasi-one-dimensional (quasi-1D) materials has allowed for detailed experimental investigations probing the physical theories that describe electronic and magnetic properties in low-dimensional solids.[1] An understanding of physical phenomena in quasi-1D solids has led to the development of a number of conducting,[1,2] superconducting,[2–4] and magnetic materials[5–7] based on low-dimensional structures. There is currently a renewed interest in quasi-1D magnetic materials as a result of the 1983 prediction by Haldane[8,9] stating that, in contrast to half-integer spin systems, there is an energy gap between the ground state and first excited state in integer spin one-dimensional Heisenberg antiferromagnets (1-D HAF).[10–19] To date, the few systems that are believed to be Haldane materials include the Ni^{2+} linear chain compounds $[Ni(C_2H_8N_2)_2NO_2]ClO_4$ (NENP),[10–15,18,20,21] $[Ni(C_3H_{10}N_2)_2NO_2]ClO_4$ (NINO),[11] $[Ni(C_3H_{10}N_2)_2N_3]ClO_4$ (NINAZ),[11,22] and $RbNiCl_3$[23] and $AgVP_2S_6$.[11] Recently, tetramethylammonium nickel nitrite,[24] $(CH_3)_4N[Ni(NO_2)_3]$ (TMNIN),[11,21,22,25] was shown to possess proper-

* To whom correspondence should be addressed.

® Abstract published in *Advance ACS Abstracts,* October 1, 1994.

(1) *Extended Linear Chain Compounds*; Miller, J. S., Ed.; Plenum Press: New York, 1983.
(2) Cowan, D. O.; Wiygul, F. M. *Chem. Eng. News* **1986**, July 21, 28–45.
(3) *Organic Superconductivity*; Kresin, V. Z., Little, W. A., Eds.; Plenum Press: New York, 1990; p 386.
(4) Adrian, F. J.; Cowan, D. O. *Chem. Eng. New* **1992**, 24–41.
(5) Kahn, O.; Pei, Y.; Nakatani, K.; Journaux, Y.; Sletten, J. *New J. Chem.* **1992**, *16*, 269–276.
(6) Miller, J. S.; Epstein, A. J.; Reiff, W. M. *Chem. Rev.* **1988**, *88*, 201–220.
(7) Caneschi, A.; Gatteschi, D.; Sessoli, R.; Rey, P. *Acc. Chem. Res.* **1989**, *22*, 392–398.
(8) Haldane, F. D. M. *Phys. Lett.* **1983**, *93A*, 464–468.
(9) Haldane, F. D. M. *Phys. Rev. Lett.* **1983**, *50*, 1153–1156.
(10) Affleck, I. *J. Phys. Condens. Matter* **1989**, *1*, 3047–3072.
(11) Renard, J. P.; Gadet, V.; Regnault, L. P.; Verdaguer, M. *J. Magn. Magn. Mater.* **1990**, *90*, 213–216.
(12) Halperin, B. I. *J. Magn. Magn. Mater.* **1992**, *104–107*, 761–765.
(13) Brunel, L. C.; Brill, T. M.; Zaliznyak, I.; Boucher, J. P.; Renard, J. P. *Phys. Rev. Lett.* **1992**, *69*, 1699–1702.
(14) Avenel, O.; Xu, J.; Xia, J. S.; Xu, M.-F.; Andraka, B.; Lang, T.; Moyland, P. L.; Ni, W.; Signore, J. C.; van Woerkens, C. M. C. M.; Adams, E. D.; Ihas, G. G.; Meisel, M. W.; Nagler, S. E.; Sullivan, N. S.; Takano, Y.; Talham, D. R.; Goto, T.; Fujiwara, N. *Phys. Rev. B* **1992**, *46*, 8655–8658.
(15) Ma, S.; Broholm, C.; Reich, D. H.; Sternlieb, B. J.; Erwin, R. W. *Phys. Rev. Lett.* **1992**, *69*, 3571–3574.
(16) Golinelli, O.; Jolicoeur, T.; Lacaze, R. *Phys. Rev. B* **1992**, *45*, 9798–9805.
(17) Mikeska, H. J. *Europhys. Lett.* **1992**, *19*, 39–44.
(18) Affleck, I. *Phys. Rev. B* **1992**, *46*, 9002–9008.
(19) Affleck, I.; Wellman, G. F. *Phys. Rev. B* **1992**, *46*, 8934–8953.
(20) Renard, J. P.; Verdaguer, M.; Regnault, L. P.; Erkelens, W. A. C.; Rossat-Mignod; Ribas, J.; Stirling, W. G.; Vettier, C *J. Appl. Phys.* **1988**, *63*, 3538–3542.
(21) Gaveau, P.; Boucher, J. P.; Regnault, L. P.; Goto, T.; Renard, J. P. *J. Appl. Phys.* **1991**, *69*, 5956–5958.
(22) Takeuchi, T.; Hori, H.; Date, M.; Yosida, T.; Katsumata, K.; Renard, J. P.; Gadet, V.; Verdaguer, M. *J. Magn. Magn. Mater.* **1992**, *104*, 813–814.
(23) Buyers, W. J. L.; Tun, Z.; Harrison, A.; Rayne, J. A.; Nicklow, R. M. *Physica B* **1992**, *180, 181*, 222–224.

0897-4756/94/2806-2051$04.50/0

ties which are consistent with a Haldane gap; however, the structure of TMNIN has never been clarified. On the basis of IR, X-ray absorption, and X-ray diffraction studies, Gadet et al.[25] were able to determine that the TMNIN structure consists of infinite chains of Ni^{2+} ions separated from one another by channels of tetramethylammonium cations. Adjacent metal ions within a chain are bridged by three nitrite ligands where the mode of bridging is Ni−N(O)O−Ni and is cis with respect to the N−O bond (cis-μ-nitro).[26] However, due to structural disorder or possible crystal twinning, the structure was not resolved with certainty. As part our investigations of 1D-HAF materials,[14] we have prepared samples of TMNIN and report here on its crystal structure determination which shows that the one-dimensional chains are comprised of alternating NiO_6 and NiN_6 octahedra. We also present magnetic susceptibility data as a function of sample orientation for TMNIN from 1.8 to 300 K and comment on the relevance of the alternating chain structure with respect the Haldane gap.

Experimental Section

Tetramethylammonium Nickel Nitrite (TMNIN, 1). Tetramethylammonium nickel nitrite, $(CH_3)_4N[Ni(NO_2)_3]$, was prepared according to the procedure described by Goodgame and Hitchman.[27] Crystals suitable for structure determination were obtained by slowly adding a solution of 0.11 g (5×10^{-4} mol) of $NiBr_2$ and 0.077 g (5×10^{-4} mol) of $(CH_3)_4NBr$ in 0.6 mL of H_2O on top of a solution of 0.33 g (5×10^{-3} mol) of $NaNO_2$ in 1.0 mL of H_2O. After 4−6 days at room temperature, the yellow-brown crystals formed on the sides of the test tube. Crystals were rinsed with cold water and dried overnight in a desiccator. Anal. Calcd for $C_4H_{12}N_4NiO_6$: C, 17.73; H, 4.43; N, 20.68. Found: C, 17.65; H, 4.49; N, 20.54.

Crystallographic Data Collection and Structure Determination. For the structure reported here, a very small yellow crystal of dimensions 0.30 mm × 0.04 mm × 0.04 mm was chosen to avoid selecting a multiple crystal. Data were collected at room temperature on a Siemens R3m/V diffractometer equipped with a graphite monochromator utilizing Mo Kα radiation (λ = 0.710 73 Å). A total of 32 reflections with $20.0° < 2\theta < 22.0°$ were used to refine the cell parameters, and 2497 reflections were collected using the ω-scan method. Four reflections ($2\bar{3}1$, $\bar{3}0\bar{2}$, $\bar{2}3\bar{1}$, 302) were measured every 96 reflections to monitor instrument and crystal stability (maximum correction on I was <1%). Absorption corrections were applied based on measured crystal faces using SHELXTL plus;[28] absorption coefficient, μ = 1.93 mm^{-1} (minimum and maximum transmission factors are 0.613 and 0.931, respectively). Examination of equivalent reflections showed that the crystal system is trigonal and that the Laue group is $P\bar{3}m$. A set of data ($h\pm k\pm l$) was collected, and the structure was solved in the space group $P\bar{3}m1$ using the heavy atom method in SHELXTL plus[28] from which the location of the Ni atoms (in special positions along the c axis; 000 and 001/2) were obtained. The rest of the non-H atoms were obtained from a subsequent Difference Fourier map. The structure was refined in SHELXTL plus using full-matrix least-squares. The non-H atoms were treated anisotropically and the H atoms were refined with isotropic thermal parameters. In the final cycle of refinement, 359 reflections with $I > 2\sigma(I)$ and 45 parameters yielded values for R and wR of 0.0250 and 0.0282, respectively. The linear absorption coefficient was calculated from values from the *International Tables for X-ray Crystallography*.[29] Scattering factors for non-hydrogen atoms were taken from Cromer and Mann[30] with anomalous-dispersion corrections from Cromer and Liberman,[31] while those of hydrogen atoms were from Stewart et al.[32] Crystal data are presented in Table 1. Fractional coordinates and isotropic thermal parameters for the non-H atoms are given in Table 2, and bond lengths and angles are given in Table 3.

Table 1. Crystallographic Data for 1

A. Crystal Data (293 K)	
a, Å	9.1029(9)
b, Å	9.1029(9)
c, Å	7.0816(7)
α, deg	90
β, deg	90
γ, deg	120
V, Å^3	508.18(8)
d_{calc}, g cm^{-3} (293 K)	1.770
empirical formula	$[(CH_3)_4N][Ni(NO_2)_3]$
formula wt, g	270.89
crystal system	trigonal
space group	$P\bar{3}m1$
Z	2
F(000), electrons	280
crystal size (mm^3)	0.30 × 0.04 × 0.04
B. Data Collection (293 K)	
radiation, λ (Å)	Mo Kα, 0.710 73
mode	ω scan
scan range	symmetrically over 1.2° about K$\alpha_{1,2}$ maximum
background	offset 1.0 and −1.0 in ω from K$\alpha_{1,2}$ maximum
scan rate, deg min^{-1}	2−4
2θ range, deg	3−55
rangle of hkl	$0 \le h \le 11$ $-11 \le k \le 11$ $-9 \le l \le 9$
total reflections measured	2497
unique reflections	472
absorption coeff μ (Mo Kα), mm^{-1}	1.93
C. Structure Refinement	
S, goodness-of-fit	0.97
reflections used, $I > 2\sigma(I)$	359
no. of variables	45
R, wR,[a] %	2.50, 2.82
R, wR,[a] all data %	4.20, 3.68
R_{int}, %	2.70
max shift/esd	0.001
min peak in diff Fourier map, e Å^{-3}	−0.33
max peak in diff Fourier map, e Å^{-3}	0.33

[a] Relevant expressions are as follows, where in the footnote F_o and F_c represent, respectively, the observed and calculated structure-factor amplitudes. Function minimized was $w(|F_o| - |F_c|)^2$, where $w = (\sigma(F))^{-2}$. $R = \Sigma(||F_o| - |F_c||)/\Sigma|F_o|$. $wR = [\Sigma w(|F_o| - |F_c|)^2/\Sigma|F_o|^2]^{1/2}$. $S = [\Sigma w(|F_o| - |F_c|)^2/(m - n)]^{1/2}$.

Magnetic Measurements. The temperature dependence of the magnetic susceptibility was obtained from magnetization measurements made with a Quantum Design (San Diego, CA) Model MPMS magnetometer operating at 0.5 Tesla. A 2.1 mg bundle of crystals was held together by a small quantity of "fingernail polish", and pieces of plastic straw were used as sample holder during the measurements. The magnetic signal arising from the plastic is well characterized and has been subtracted from the results. While the parasitic signal associated with the fingernail polish is not as well characterized,

(24) Chemical Abstracts index name *N,N,N*-trimethylmethanaminium tris(nitrito)nickelate(1−). Registry number 32056-13-6.

(25) Gadet, V.; Verdaguer, M.; Briois, V.; Gleizes, A.; Renard, J. P.; Beauvillain, P.; Chappert, C.; Goto, T.; Le Dang, K.; Veillet, P. *Phys. Rev. B* **1991**, *44*, 705−712.

(26) Hitchman, M. A.; Rowbottom, G. L. *Coord. Chem. Rev.* **1982**, *42*, 55−132.

(27) Goodgame, D. M. L.; Hitchman, M. A. *Inorg. Chem.* **1967**, *6*, 813−816.

(28) Sheldrick, G. M. SHELXTL plus; Nicolet XRD Corp.: Madison, WI, 1990.

(29) *International Tables for X-ray Crystallography*; Kynoch Press: Birmingham, 1974; Vol. IV.

(30) Cromer, D. T.; Mann, J. B. *Acta Crystallogr.* **1968**, *A24*, 321−324.

(31) Cromer, D. T.; Liberman, D. *J. Phys. Chem.* **1970**, *53*, 1891−1898.

(32) Stewart, R. F.; Davidson, D. R.; Simpson, W. T. *J. Chem. Phys.* **1965**, *42*, 3175−3187.

Table 2. Fractional Coordinates and Equivalent Isotropic[a] Thermal Parameters (Å²) for the Non-H Atoms of Compound I

atom	x	y	z	U
ni1	0.0	0.0	0.0	0.0238(2)
Ni2	0.0	0.0	0.5	0.0254(3)
N1	0.2192(3)	0.1096(2)	0.1661(3)	0.024(1)
O1	0.2193(3)	0.1097(1)	0.3468(3)	0.031(1)
O2	0.3585(3)	0.1793(1)	0.0923(3)	0.043(1)
N2	0.3333	0.6667	0.3492(6)	0.027(1)
C1	0.3333	0.6667	0.5604(8)	0.041(2)
C2	0.4225(3)	0.8451(5)	0.2808(7)	0.044(2)

[a] For anisotropic atoms, the U value is U_{eq}, calculated as $U_{eq} = {}^1/_3\sum_i \sum_j U_{ij} a_i^* a_j^* A_{ij}$ where A_{ij} is the dot product of the ith and jth direct space unit cell vectors.

Table 3. Selected Bond Lengths (angstroms) and Angles (degrees) for the Non-H Atoms of Compound I[a]

1	2	3	1–2	1–2–3
N1	Ni1	N1a	2.090(2)	180.00(0)
N1	Ni1	N1b		91.44(8)
N1	Ni1	N1c		88.56(8)
N1	Ni1	N1d		91.44(6)
N1	Ni1	N1e		88.56(6)
O1	Ni2	O1a	2.041(2)	180.00(0)
O1	Ni2	O1b		85.62(5)
O1	Ni2	O1c		94.38(5)
O1	Ni2	O1d		85.62(7)
O1	Ni2	O1e		94.38(7)
O1	N1	O2	1.280(3)	115.4(2)
O1	N1	Ni1		124.3(2)
O2	N1	Ni1	1.218(3)	120.3(2)
Ni2	O1	N1		122.1(2)
C1	N2	C2	1.495(7)	109.0(2)
C1	N2	C2a		109.0(2)
C2	N2	C2a	1.487(4)	109.9(3)
C2	N2	C2b		109.9(3)
C2a	N2	C2b	1.487(4)	109.9(3)
C2b	N2	C1	1.487(4)	109.0(2)

[a] N1x and O1x, where x = a, b, c, d, e, are derived from N1 and O1, respectively, using the $\bar{3}$ symmetry operator. C2a and C2b are derived from C2 by applying the 3-fold rotation symmetry at ${}^1/_3$, ${}^2/_3$, z.

this contribution has been estimated from measurements of large samples possessing a known response and has been subtracted.

Results and Discussion

TMNIN Structure. The structure consists of infinite chains of Ni atoms along the c axis, Figure 1, linked by bridging NO_2 ligands such that alternate Ni ions along a chain are chemically distinct with Ni1 octahedrally coordinated with six nitrite nitrogens, and the adjacent Ni2 octahedrally coordinated with six nitrite oxygens. The Ni ions are evenly spaced along the chain and are separated by one-half the cell edge or 3.541 Å. The tetramethylammonium ions are located in positions along the 3-fold rotation axes where the N atoms occupy positions ${}^1/_3$, ${}^2/_3$, z and ${}^2/_3$, ${}^1/_3$, z', with one C atom on the 3-fold rotation axis and another on the mirror plane passing through the 3-fold axis. The counterions separate the Ni chains, and the closest interchain Ni–Ni distance is equal to the cell edge of 9.1029 Å. A packing diagram, showing the location of the tetramethylammonium counterions and the interchain separations, is given in Figure 2.

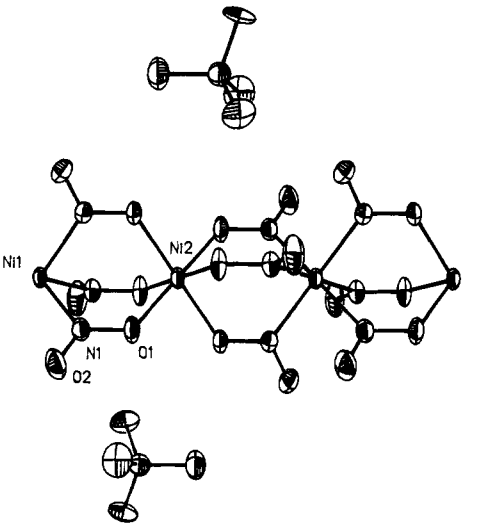

Figure 1. View perpendicular to the c axis of a portion of the Ni chain in TMNIN. Alternating Ni sites are octahedrally coordinated by N atoms (Ni1) and O atoms (Ni2) of the bridging nitrite ligands. Nickel chains are separated by columns of tetramethylammonium counterions. Two tetramethylammonium ions from different columns are shown; others are omitted for clarity. Atoms are represented by 50% probability ellipsoids.

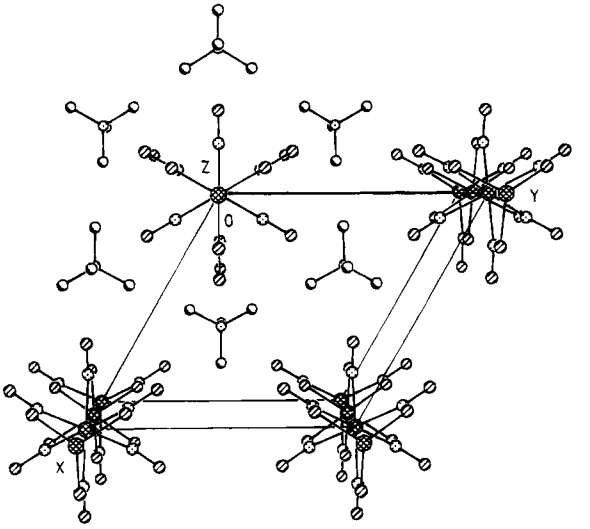

Figure 2. Packing diagram for TMNIN viewed along the c axis showing the separated nickel chains. Intrachain Ni–Ni distances are 3.541 Å, while the interchain distance is 9.1029 Å.

The nitrite geometry is consistent with that found in other *cis*-μ-nitro nickel complexes,[26,33–35] with the bond from nitrogen to the bonding oxygen longer than the bond to the nonbonding oxygen. The ONO bond angle is 115°. The nonligating nitrite O atoms are closer to the nitrogen-coordinated Ni1 than to the oxygen-coordinated Ni2 and form a space for the tetramethylammonium ions. Since the two Ni ions are chemically inequivalent, the tetramethylammonium ions lie closer to the oxygen-coordinated nickel (N–Ni2 distance is 5.363 Å) than to the nitrogen-coordinated nickel (N–Ni1 distance is 5.809 Å). The NiN_6 and NiO_6 octahedra

(33) Finney, A. J.; Hitchman, M. A.; Raston, C. L.; Rowbottom, G. L.; White, A. H. *Aust. J. Chem.* **1981**, *34*, 2125–2138.
(34) Finney, A. J.; Hitchman, M. A.; Raston, C. L.; Rowbottom, G. L.; White, A. H. *Aust. J. Chem.* **1981**, *34*, 2139–2157.
(35) Finney, A. J.; Hitchman, M. A.; Raston, C. L.; Rowbottom, G. L.; White, A. H. *Aust. J. Chem.* **1981**, *34*, 2159–2176.

are distorted, as shared faces along the chain slightly flatten each octahedron. The distortion is less in the NiN_6 octahedron to minimize crowding of the nonbonding nitrite oxygens. This is in contrast to the axial distortion seen in the hexagonal $MNiX_3$ (M = Cs, Rb, $N(CH_3)_4$; X = Cl, Br) compounds that are also comprised of 1D chains formed from face-sharing octahedra.[36,37] In the $MNiX_3$ series, the MX_6 octahedra are elongated along the chain axis in order to minimize the Ni–Ni Coulomb repulsions.[36,37] In TMNIN, each NO_2 plane bisects the angle between the perpendicular axes of the NiN_6 and NiO_6 octahedron that it coordinates. Normally, in nitrite binding, the NO_2 plane is parallel to one of the perpendicular axes in order to maximize π-overlap with the metal.[26,38,39] The poor metal–ligand π-overlap in TMNIN is consistent with its low value of magnetic exchange[25] ($J/k_B \approx -10$ K, see below) despite the short Ni–Ni distance. For comparison, in NENP where the bridging NO_2 ligand is aligned for good π-overlap, $J/k_B = -48$ K, despite the longer Ni–Ni separation of 5.15 Å.[11,20,40]

Magnetic Susceptibility. Susceptibility vs temperature data from 1.8 to 300 K for a 2.1 mg bundle of single crystals, aligned with their chain axes parallel, are presented in Figure 3 for two orientations of the bundle with respect to the magnetic field. A background contribution has been subtracted to account for the diamagnetic contributions of the sample, the sample holder, and the commercial "fingernail polish" that was used to hold the bundle of crystals together. The susceptibility rises as the temperature decreases, reaching a maximum around 14 K, and then sharply decreases down to 1.8 K. The shape of the susceptibility plot is similar to that seen for a multicrystalline sample[25] and is characteristic of a Haldane gap system with the susceptibility approaching zero as $T \rightarrow 0$.[41] The data reveal a slight anisotropy in the susceptibility for the two orientations shown in Figure 3. Above $T = 6$ K, the data are fit with an analytical expression[25,42] (eq 1) derived from the numerical studies of Weng[43] for the susceptibility of an $S = 1$ Heisenberg chain:

$$\frac{X_M kT}{N(g\mu_B)^2} = \frac{2 + 0.0194x + 0.777x^2}{3 + 4.346x + 3.232x^2 + 5.834x^3} \quad (1)$$

where $x = J/kT$.[44] Weng's results[43] are based on the simple Hamiltonian, $\mathbf{H} = -J\sum \mathbf{S}_i\mathbf{S}_{i+1}$, and ignore the signal ion anisotropy terms $D(\mathbf{S}_i^z)^2$ and $E\{(\mathbf{S}_i^x)^2 - (\mathbf{S}_i^y)^2\}$ that represent the axial and rhombic distortions from cubic symmetry, respectively. Nonlinear least-squares fits of the data for $T > 6$ K yield, for $H_\parallel$ c axis, $g_\parallel = 2.088 \pm .005$, $J/k_B = -10.11 \pm 0.05$ K, and for $H_\perp c$ axis, $g_\perp = 2.091 \pm .004$, $J/k_B = -10.40 \pm 0.04$ K where the listed uncertainties are 1σ statistical errors derived from the fitting procedure and do not represent systematic errors that may be present in the data, such as those related to the subtraction of the background contributions.

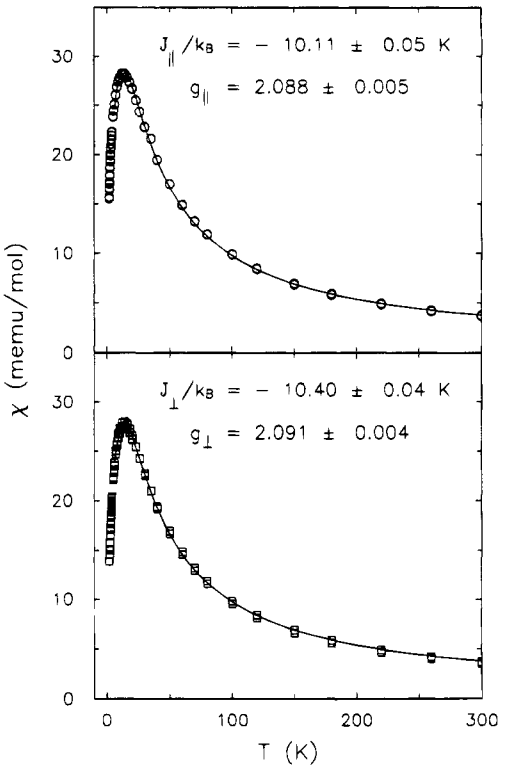

Figure 3. Magnetic susceptibility, χ, is plotted as a function of temperature, T, for the cases where the magnetic field of 0.5 T is oriented parallel (top) and perpendicular (bottom) to the TMNIN chain axis. The background contributions have been subtracted as explained in the text. Using eq 1, a nonlinear least-squares fit of the data for $T \geq 6$ K yields the solid curves for the values of g and J that are listed.

To date, there is no explicit expression for the temperature-dependent susceptibility of a linear chain $S = 1$ Heisenberg antiferromagnet over a broad temperature range that includes the single ion anisotropy terms. However, the axial distortion parameter, D, for a trigonal or tetragonal distortion can be estimated from the orientational difference in g values according to the expression[20,45]

$$D = \lambda/2(g_\parallel - g_\perp) \quad (2)$$

where λ is the spin–orbit coupling parameter. By using the g values determined from the fits to the susceptibility data in Figure 3 and taking λ as −360 K,[20,45] a coarse estimate of $D/k_B = 0.5 \pm 1.2$ K is obtained. This value is only an estimate, but is consistent with recent EPR work which places an upper bound on $|D|$ to be less than 1 K.[46]

(36) Stucky, G.; D'Agostino, S.; McPherson, G. *J. Am. Chem. Soc.* **1966**, *88*, 4828–4831.
(37) Asmussen, R. W.; Kindt Larsen, T.; Soling, H. *Acta Chem. Scand.* **1969**, *23*, 2055–2060.
(38) Takagi, S.; Joesten, M. D.; Lenhert, P. G. *Acta Crystallogr.* **1975**, *B31*, 1968–1970.
(39) Takagi, S.; Joesten, M. D.; Lenhert, P. G. *Acta Crystallogr.* **1975**, *B31*, 1970–1972.
(40) Goodgame, D. M.; Hitchman, M. A.; Marsham, D. F. *J. Chem. Soc. A* **1971**, 259–264.
(41) The expected χ vs T behavior for a gapless 1-D HAF was determined by a number of workers including Weng,[43] who showed that χ_0/χ_{max} for $S = 1$ should lie between 0.69 ($S = 1/2$) and 0.80 ($S = \infty$). In Figure 3, data are plotted to 1.8 K where already $\chi_{1.8}/\chi_{max} \approx 0.5$.
(42) Meyer, A.; Gleizes, A.; Girerd, J. J.; Verdaguer, M.; Kahn, O. *Inorg. Chem.* **1982**, *21*, 1729–1739.
(43) Weng, C. Y. Thesis, Carnegie Mellon University, 1968.
(44) Equation 1 is an analytical expression of Weng's results that is valid only for $T \geq J/2k_B$. At these temperatures, the effect of an energy gap on the susceptibility should be small, and eq 1 can be used to fit the data and obtain an estimate of J/k_B and g.
(45) Abragam, A.; Bleaney, B. *Electron Paramagnetic Resonance of Transition Metal Ions*; Clarendon Press: Oxford, 1970; p 911.
(46) Koido, N.; Kambe, T.; Teraoka, S.; Hirai, S.; Goto, T.; Chou, L.-K., Talham, D. R.; Meisel, M. W.; Nagata, K., to be published.

Alternating Site Structure. The structure determination shows that TMNIN differs from most other materials[47] thought to possess a Haldane gap in that the 1D chains consist of alternating Ni sites that are chemically distinct. While nearest-neighbor exchange, J, along the chain is constant, the next-nearest-neighbor coupling, $J_{\parallel}$, alternates in the chain, and two parameters, $J_{\parallel_1}$ and $J_{\parallel_2}$, are required to describe the next-nearest-neighbor interactions, as shown schematically below:

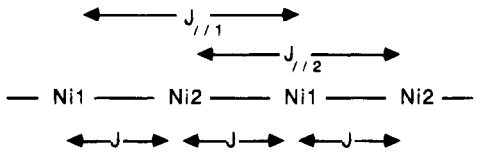

The situation in TMNIN can be contrasted to "dimerized" alternating linear chains where there are two alternating nearest-neighbor exchange interactions; each site experiences a nearest-neighbor exchange interaction, J, with one of its neighbors, and a second interaction, αJ, with its other nearest neighbor. TMNIN, on the other hand, is well characterized by one nearest-neighbor interaction, and there is no evidence for any low-temperature structural transition that might introduce a dimerization.

To date, the signs and magnitudes of the next-nearest neighbor and interchain interactions have not been established, nor have discrete g values for the two different nickel sites been observed. However, the existence of the alternating sites raises the question of whether or not TMNIN is expected to be a Haldane gap material. Tonegawa et al.[48] have numerically studied the properties of an isotropic $S = 1$ 1D-HAF with competing interactions. These workers find that antiferromagnetic next-nearest-neighbor interactions stabilize the Haldane phase. Therefore, if $J_{\parallel_1}$ and $J_{\parallel_2}$ are both antiferromagnetic in nature, then the Haldane gap for TMNIN should be well established. On the other hand, if either or both of the next-nearest-neighbor interactions is ferromagnetic, then the ground state of the system is not obvious, although one might expect it to be more ordered.

The models used here to fit the susceptibility data are not able to discern differences between $J_{\parallel_1}$ and $J_{\parallel_2}$, and it is probable that next-nearest neighbor interactions are too small to influence the magnetic properties in the temperature region investigated to date. A similar interpretation has recently been made by Landee et al.[47] in studies of $[Ni(C_2H_8N_2)_2NO_2]PF_6$ (NENF) which is another linear chain material with two distinct Ni sites. For TMNIN, the low value of the susceptibility as $T \rightarrow 0$, is consistent with an energy gap between the ground state and magnetically excited states.[25] In addition, field-dependent magnetization[22,25] and nuclear magnetic relaxation studies[21] on powdered samples also give evidence that a gap exists in TMNIN.

Acknowledgment. We acknowledge fruitful conversations with S. E. Nagler during the course of this work, and we are grateful to G. R. Stewart for making the magnetometer available to us. Research support has been provided by the National Science Foundation [DMR-9205333] (D.R.T.) and [DMR-9200671] (M.W.M.).

Supplementary Material Available: Complete crystallographic data, complete table of bond lengths and angles for the non-hydrogen atoms, anisotropic thermal parameters for the non-hydrogen atoms, fractional coordinates and isotropic thermal parameters for the hydrogen atoms, and bond lengths and angles to the hydrogen atoms of TMNIN (2 pages); observed and calculated structure factors for **1** (2 pages). Ordering information is given on any current masthead page.

(47) Landee, C. P.; Reza, K. A.; Bond, M. R., Willett, R. D.; Ferré, J.; Jamet, J.-P., to be published.

(48) Tonegawa, T.; Kaburagi, M.; Ichikawa, N.; Harada, I. *J. Phys. Soc. Jpn.* **1982**, *61*, 2890–2900.